Laser and Particle Beams (2017), *35*, 19–25.

doi:10.1017/S0263034616000720

Effect of the axial magnetic field on coexisting stimulated Raman and Brillouin scattering of a circularly polarized beam

ASHISH VYAS, SWATI SHARMA, RAM KISHOR SINGH, AND R.P. SHARMA
Centre for Energy Studies, IIT Delhi, Delhi, 110016, India
(RECEIVED 19 June 2016; ACCEPTED 22 October 2016)

Abstract

This paper presents a model to study the two prominent coexisting instabilities, stimulated Raman (SRS), and stimulated Brillouin scattering (SBS) in the presence of background axial magnetic field. In the context of laser-produced plasmas, this model is very useful in the situations where a self-generated axial magnetic field is present as well as where an external axial magnetic field is applied. Due to the interplay between both the scattering processes, the behavior of one scattering process is greatly modified in the presence of another coexisting scattering process. The impact of this coexisting phenomenon and axial magnetic field on the back reflectivity of scattered beams has been explored. It has been demonstrated that the back reflectivity gets modified significantly due to the coexistence of both the scattering processes (SRS and SBS) as well as due to the axial magnetic field. Results are also compared with the three-wave interaction case (isolated SRS or SBS case).

Keywords: Stimulated Brillouin scattering; Stimulated Raman scattering

1. INTRODUCTION

Recently, the interaction of intense electromagnetic waves (laser beams) with plasmas has attracted a great deal of attention. The motivation for such studies is because of its application in various research fields such as inertial confinement fusion (ICF) (Lindl *et al.*, 2004), laboratory astrophysics (Remington *et al.*, 1999), X-ray lasers (Li *et al.*, 2011), compact laser-driven accelerators (Tajima & Dawson, 1979; Wang *et al.*, 2000), pulsar electrodynamics (Harding & Lai, 2006), higher harmonic generation (Baeva *et al.*, 2006), and many more (Tajima & Mourou, 2002). The success of laser–plasma interaction critically depends on the coupling of the incident laser energy to the plasma. Mainly, laser deposited its energy in the plasma through resonant absorption in which laser beam must reach up to critical density for effective coupling. Various instabilities that arise during the laser–plasma interaction are of crucial importance for the coupling efficiency. These instabilities reduce the coupling efficiency by scattering a large fraction of the incident laser energy and hot electron generation in the vicinity of critical density. Among various parametric instabilities stimulated Raman and Brillouin scattering (SRS and SBS, respectively) are particularly important in context to laser–plasma interaction and they both involve decay of the incident electromagnetic wave into a scattered electromagnetic wave and a longitudinal wave. The daughter longitudinal waves are electron plasma waves (EPW) in the case of SRS, and the ion acoustic waves (IAW) in the case of SBS (Kruer, 1974; Chen, 1984; Liu & Tripathri, 1994). The excitation of both Raman and Brillouin instabilities can yield poor coupling of laser energy to the plasma by scattering a significant amount of incident laser energy, as well as the generation of hot electrons (mainly due to SRS), which damage the uniformity of energy deposition and also lead to significant plasma pre-heating (Guérin *et al.*, 1998; Lindl *et al.*, 2004). Therefore, both SRS and SBS do greatly affect the coupling efficiency and studies of these instabilities are of extreme importance.

It is well established both theoretically and experimentally that there exists a self-generated magnetic field in laser-produced plasmas whose magnitude is up to a few hundred megagauss (Sentoku *et al.*, 1999; Nicolaï *et al.*, 2000; Sandhu *et al.*, 2002; Mondal *et al.*, 2012). Apart from the self-generated magnetic field, in many situations an external

Address correspondence and reprint requests to: R.K. Singh, Centre for Energy Studies, IIT Delhi, Delhi, 110016, India. E-mail: ram007kishor@gmail.com

magnetic field may also be applied (Perkins, 1977; Hellsten & Villard, 1988). The magnetic field can be perpendicular or along the direction of propagation of incident laser beam. In the former case, the dispersion relations of both the electromagnetic wave (pump) and the plasma wave gets modified due to the magnetic field, while in the latter case only the pump is affected. In this paper, we have restricted ourselves to the latter case only, that is, the propagation of an electromagnetic wave along the direction of static background magnetic field. In this typical case, the principal wave is a circularly polarized wave (Chen, 1984). Earlier, a lot of study has been done on self-generated axial magnetic field (Briand *et al.*, 1985; Srivastava *et al.*, 1992; Khan *et al.*, 1998*a*, *b*; Nijmudin *et al.*, 2001). Nijmudin *et al.* (2001) have observed axial magnetic field of the order of 7 MG with high spatial and temporal precision during interaction of a circularly polarized laser pulse with an under dense plasma. Khan *et al.* (1998*a*, *b*) experimentally estimated the self-generated axial magnetic field by measuring the change in the polarization of stimulated Brillouin scattered (SBS) radiation as compared to the incident laser radiation. This magnetic field plays a very crucial role in laser–plasma interaction by modifying the dispersion relation of waves in plasma, and hence both the scattering processes (SRS and SBS) and hot electron generation get affected by this self-generated magnetic field. Therefore, for the better understanding of laser–plasma interaction it is necessary to study these stimulated scattering processes (SRS and SBS) in the presence of the magnetic field.

In the past, an extensive theoretical and numerical study has been carried out for both SRS and SBS processes in the magnetized plasma, but without considering the interplay among them (Guérin *et al.*, 1995; Barr *et al.*, 1998; Mahmoud & Sharma, 2001; Shuller & Porzio, 2010; Paknezhad, 2012). However, both the processes can coexist up to n_{cr} (critical density) in the magnetized plasma. Due to this interplay between both the scattering processes, one scattering process explicitly affects the other process and in addition to that the process of hot electron generation also gets affected significantly (Sharma & Dragila, 1988). Although, the coexistence phenomenon of both the scattering processes (SRS and SBS) has been experimentally observed (Walsh *et al.*, 1984; Labaune *et al.,* 1997; Michel *et al.*, 2010) as well as studied theoretically (Kolber *et al.*, 1995; Hao *et al.*, 2013; Sharma *et al.*, 2013; Vyas *et al.*, 2014*a*, *b*). In the unmagnetized plasma, Vyas *et al.* (2014*a*, b) and Sharma *et al.* (2013) have theoretically observed the impact of the coexistence phenomenon on the back reflectivity of scattered beams (SRS and SBS) at relativistic laser power and relatively low laser powers, respectively. They have found that the back-reflectivities of both the scattered beams get modified significantly due to this coexistence. Recently, Vyas *et al.* (2016) have theoretically studied the interplay between SRS and SBS of an extraordinary electromagnetic wave propagating perpendicular to the static background magnetic field. But the effect of the axial magnetic field has not been considered so far. In a recent experimental work (Montgomery *et al.*, 2015), it is observed that by applying an external magnetic field, the laser–energy coupling to the hohlraum targets gets increased. Therefore, in order to understand the coupling of laser energy with magnetized plasma, it is necessary to study this coexistence phenomenon in the presence of the axial magnetic field.

In the present paper, we have simultaneously studied the SRS and SBS processes in collisionless plasma in the presence of an axial magnetic field. We have investigated the effect of magnetic field on the coexistence of SRS and SBS of both right- as well as left circularly polarized electromagnetic wave propagating along the static background magnetic field. We have derived and simulated the back reflectivity of both the scattering processes to get the estimate about the scattered energy due to this coexistence phenomenon as well as due to the presence of magnetic field. It has been found that the gain factors and consequently the back-reflectivities of SRS and SBS significantly modified due to both coexistence phenomenon as well as the background axial magnetic field.

This paper is arranged as follows. In Section 1, we have presented a three-dimensional theoretical model to study SRS and SBS simultaneously (five wave interaction 5WI) and derived the expression for the back reflectivity of the both the scattered beams in the presence of background axial magnetic field. Section 3 presents the detailed discussion of the results followed by the conclusion in Section 4.

2. MODEL EQUATION

Consider homogenous plasma immersed in a strong static magnetic field $B_0^0\hat{z}$. A circularly polarized high-power laser beam $\vec{E}_0$ is used as a pump having frequency ω_0 and wave number k_0, propagating through the plasma along the z-axis, that is, along the magnetic field $B_0^0\hat{z}$. The circularly polarized pump laser beam $\vec{E}_0$ can be either right- or left-circularly polarized:

$$\vec{E}_{0r} = E_{00}(\hat{x} + i\hat{y})\exp[-i(\omega_0 t - k_0 z)], \tag{1a}$$

$$\vec{E}_{0l} = E_{00}(\hat{x} - i\hat{y})\exp[-i(\omega_0 t - k_0 z)]. \tag{1b}$$

Here $\vec{E}_{0r}$ and $\vec{E}_{0l}$ represent the right- and left-hand circularly polarized waves, respectively. Frequency ω_0 and wave number k_0 of the pump are related by dispersion relation (Chen, 1984):

$$\frac{c^2k_0^2}{\omega_0^2} = 1 - \frac{\omega_P^2}{\omega_0(\omega_0 \mp \omega_c)}. \tag{2}$$

Here "−" and "+" sign is for the right- and left-hand circularly polarized waves, respectively, $\omega_c = eB_0^0/m_e c$ is the electron cyclotron frequency. This pump wave interacts with the plasma in the presence of background magnetic

https://doi.org/10.1017/S0263034616000720 Published online by Cambridge University Press

field and decays into scattered electromagnetic waves (SRS and SBS) and the electrostatic waves (EPW and IAW). One may write the total electric field $\vec{E}$ inside the plasma as:

$$\vec{E} = \vec{E}_0 + \vec{E}_R + \vec{E}_B, \tag{3}$$

where $\vec{E}_0$ $\vec{E}_0$, $\vec{E}_R$, and $\vec{E}_B$ are the electric field of the incident wave, SRS wave, and SBS wave, respectively. Our main concern is to study the interplay between these three EM waves. In this 5WI model (pump wave, SRS wave, SBS wave, EPW, and IAW) the phase-matching condition is given as follows:

$$\vec{k}_0 = \vec{k}_R + \vec{k}_L, \vec{k}_0 = \vec{k}_B + \vec{k}_A \text{ and } \omega_0 = \omega_R + \omega_L, \omega_0 = \omega_B + \omega_A, \tag{4}$$

where $\vec{k}_\alpha$ and ω_α ($\alpha = 0$, R, B, L, A) are the wave number and frequency of the pump wave, SRS wave, SBS wave, EPW, and IAW, respectively. The governing wave equation for the total electric field $\vec{E}$ inside the plasma can be written (Sodha *et al.*, 1976) in term of the total current density $\vec{J}$ as follows:

$$\vec{\nabla}^2\vec{E} + \vec{\nabla}(\vec{\nabla}\cdot\vec{E}) = \frac{1}{c^2}\frac{\partial^2\vec{E}}{\partial t^2} + \frac{4\pi}{c^2}\frac{\partial\vec{J}}{\partial t}, \tag{5}$$

where

$$\omega_p^2 = \left(\frac{4\pi n_0 e^2}{m_e}\right), \omega_c = \frac{eB_0^0}{m_e c} \text{ and } \omega_{uh}^2 = \omega_p^2 + \omega_c^2. \tag{6}$$

Here $\vec{V}_\alpha(\alpha = 0, R, B)$ is the field induced velocity by which the electrons oscillate in the field $\vec{E}_\alpha(\alpha = 0, R, B)$, respectively. Here, N_0 represents the background plasma electron density, N_{eR} and N_{eB} are the electron density perturbations in the EPW and IAW, respectively. The components of $\vec{V}_\alpha(\alpha = 0, R, B)$ are given by:

$$\vec{V}_\alpha = \frac{-ie}{m(\omega_\alpha \mp \omega_c)}\vec{E}_\alpha. \tag{7}$$

Here "−" and "+" sign is for right- and left-hand circularly polarized waves, respectively, e and m_e are the electron charge and mass respectively and c is the speed of light. Using Eqs (6) and (7) in Eq. (5), one can obtain the equations governing the pump and scattered beams as follows:

$$\nabla^2\vec{E}_0 + \frac{\omega_0^2}{c^2}\left[1 - \frac{\omega_p^2}{\omega_0(\omega_0 \mp \omega_c)}\right]\vec{E}_0 = \frac{-4\pi e}{c^2}\frac{1}{2}\frac{\partial}{\partial t}(N_{eR}\vec{V}_R + N_{eB}\vec{V}_B), \tag{8}$$

$$\nabla^2\vec{E}_R + \frac{\omega_R^2}{c^2}\left[1 - \frac{\omega_p^2}{\omega_R(\omega_R \mp \omega_c)}\right]\vec{E}_R = \frac{-4\pi e}{c^2}\frac{1}{2}\frac{\partial}{\partial t}(N_{eR}^*\vec{V}_0), \tag{9}$$

$$\nabla^2\vec{E}_B + \frac{\omega_B^2}{c^2}\left[1 - \frac{\omega_p^2}{\omega_B(\omega_B \mp \omega_c)}\right]\vec{E}_B = \frac{-4\pi e}{c^2}\frac{1}{2}\frac{\partial}{\partial t}(N_{eB}^*\vec{V}_0), \tag{10}$$

where ω_p is the plasma frequency. By solving the wave dynamical equations of both the electrostatic waves (EPW and IAW), the expression for N_{eR} and N_{eB} are given by

$$\frac{N_{eR}}{N_0} = i\frac{e^2 k_R k_L|\vec{E}_0.\vec{E}_R^*|}{4m^2\Gamma_e\omega_L\omega_R(\omega_0 \mp \omega_c)}, \tag{11}$$

$$\frac{N_{eB}}{N_0} = i\frac{e^2 k_B k_A|\vec{E}_0.\vec{E}_B^*|}{4mM\Gamma_i\,\omega_A\,\omega_B(\omega_0 \mp \omega_c)}, \tag{12}$$

where, Γ_i and Γ_e are the phenomenological damping coefficients for IAW and EPW, respectively. On substituting the expressions of N_{eR}andN_{eB} in Eqs. (8)–(10), the following equations are obtained:

$$\nabla^2\vec{E}_0 + \frac{\omega_0^2}{c^2}\left[1 - \frac{\omega_p^2}{\omega_0(\omega_0 \mp \omega_c)}\right]\vec{E}_0 = \frac{ie^2\omega_p^2\omega_0}{8c^2m} \times\left[\left(\frac{k_R k_L|\vec{E}_R\vec{E}_R^*|}{m\Gamma_e\,\omega_L\omega_R(\omega_0 \mp \omega_c)(\omega_R \mp \omega_c)}\right) + \left(\frac{k_B k_A|\vec{E}_B\vec{E}_B^*|}{M\Gamma_i\,\omega_A\,\omega_B(\omega_0 \mp \omega_c)(\omega_B \mp \omega_c)}\right)\right]\vec{E}_0 \tag{13}$$

$$\nabla^2\vec{E}_R + \frac{\omega_R^2}{c^2}\left[1 - \frac{\omega_p^2}{\omega_R(\omega_R \mp \omega_c)}\right]\vec{E}_R = -ie^2\omega_p^2\left(\frac{k_R k_L|\vec{E}_0.\vec{E}_0^*|}{8m^2\omega_L(\omega_0 \mp \omega_c)^2c^2\Gamma_e}\right)\vec{E}_R \tag{14}$$

$$\nabla^2\vec{E}_B + \frac{\omega_B^2}{c^2}\left[1 - \frac{\omega_p^2}{\omega_B(\omega_B \mp \omega_c)}\right]\vec{E}_B = -ie^2\omega_p^2\left(\frac{k_B k_A|\vec{E}_0.\vec{E}_0^*|}{8Mm\omega_A(\omega_0 \mp \omega_c)^2c^2\Gamma_i}\right)\vec{E}_B \tag{15}$$

The solution can be written as

$$\vec{E}_0 = \vec{E}_0 e^{-G_0 z}, \tag{16}$$

$$\vec{E}_R = \vec{E}_R e^{-g_R z}, \tag{17}$$

$$\vec{E}_B = \vec{E}_B e^{-g_B z}, \tag{18}$$

where G_0, g_R, and g_B are the gain factors of the pump wave, SRS, and SBS respectively for the coexistence (5WI) case. Substituting the above solutions into Eqs (13)–(15) along

https://doi.org/10.1017/S0263034616000720 Published online by Cambridge University Press

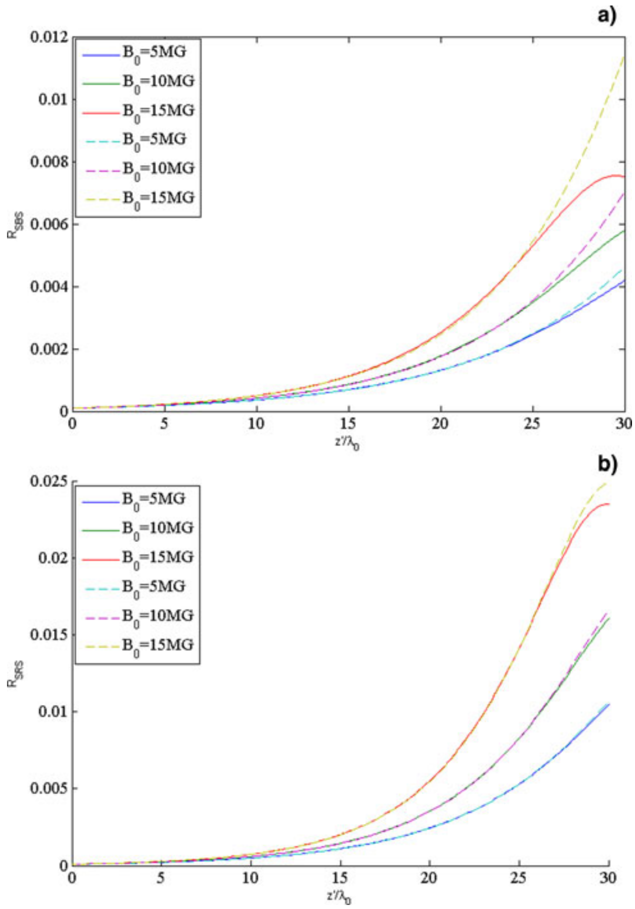

Fig. 1. Variation in the back reflectivity of *r*-mode with the distance of propagation, at different values of the axial magnetic field, (a) SBS process (R_{SBS}), (b) SRS process (R_{SRS}). The solid curve corresponds to the 5WI case and the dash curve corresponds to the 3WI case ($\omega_p = 0.15\ \omega_0$).

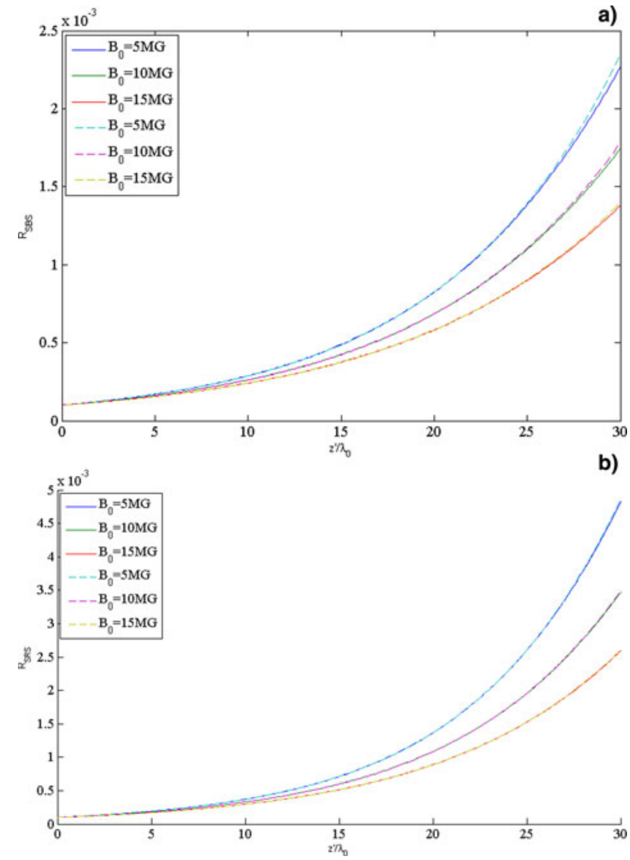

Fig. 2. Variation in the back reflectivity of *l*-mode with the distance of propagation, at different values of the axial magnetic field, (a) SBS process (R_{SBS}), (b) SRS process (R_{SRS}). The solid curve corresponds to the 5WI case and the dash curve corresponds to the 3WI case ($\omega_p = 0.15\ \omega_0$).

with the dispersion relation of EMW [Eq. (2)] we can get:

$$G_0 = \frac{e^2\omega_p^2\omega_0}{16\,c^2 m k_0}\Bigg[\left(\frac{k_R k_L\,|E_R E_R^*|}{m\,\Gamma_e\,\omega_L\omega_R(\omega_0 \mp \omega_c)(\omega_R \mp \omega_c)}\right) + \left(\frac{k_B k_A|E_B E_B^*|}{M\,\Gamma_i\,\omega_A\,\omega_B(\omega_0 \mp \omega_c)(\omega_B \mp \omega_c)}\right)\Bigg], \quad (19)$$

$$g_R = -e^2\omega_p^2\left(\frac{k_L\,|E_0.E_0^*|}{16m^2\omega_L(\omega_0 \mp \omega_c)^2 c^2\ \Gamma_e}\right), \quad (20)$$

and

$$g_B = -e^2\omega_p^2\left(\frac{k_A\,|E_0.E_0^*|}{16\,\mathrm{M}m\omega_A(\omega_0 \mp \omega_c)^2 c^2 \Gamma_i}\right). \quad (21)$$

Here "−" and "+" sign is for right and left-hand circularly polarized waves, respectively. The back reflectivity, defined as the ratio of the scattered wave intensity to the input pump wave intensity, can be expressed for the SRS and SBS wave respectively as follows:

$$R_{SRS} = \frac{|\vec{E}_R\vec{E}_R^*|}{E_{00}^2}v_{gr} = \frac{E_{0R}^2(z'=0)\,v_{gr}}{E_{00}^2}e^{-2g_R z'} \quad (22)$$

$$R_{SBS} = \frac{|\vec{E}_B\vec{E}_B^*|}{E_{00}^2} = \frac{E_{0B}^2(z'=0)}{E_{00}^2}e^{-2g_B z'} \quad (23)$$

here $z^{'} - = -L_z - z$, L_z is the interaction length and v_{gr} is ratio of the group velocity of the Raman scattered beam to the group velocity of the pump beam. In the next section, the numerical results are obtained and discussed.

3. RESULTS AND DISCUSSION

We have simulated the back-reflectivities of the scattered beams and demonstrated that how modification in back-reflectivities takes place due to the coexistence of both the scattering processes. Also demonstrate the effect of the background magnetic field on the back-reflectivities. For the numerical simulation, following set of laser–plasma parameters are chosen:

https://doi.org/10.1017/S0263034616000720 Published online by Cambridge University Press

$\lambda_0 = 1.06$ μm, Pump intensity $I = 5 \times 10^{16}$ W/cm^2, Seed beam intesities $= I \times 10^{-4}$ W/cm^2, $\Gamma_e = 8 \times 10^{-3}\omega_0$ and $\Gamma_i = 10^{-4}\omega_0$.

Furthermore, the results obtained in the absence of magnetized plasma (Sharma *et al.*, 2013) can be restored by setting the value of B_0^0 to zero and compared the results obtained in the present case (in the presence of magnetic field). The results are described in the form of graphs as below.

For the right circularly polarized mode (*r*-mode), Figure 1(a) and 1(b) shows the variation of back reflectivity of SBS and SRS with the background magnetic field, respectively. Similarly, Figure 2(a) and 2(b) shows the variation of back reflectivity of SBS and SRS with the background magnetic field, respectively, for the left circularly polarized mode (*l*-mode). The back reflectivity is plotted against the normalized distance of propagation for both 3WI and 5WI cases for $\omega_p = 0.15\ \omega_0$. The dash curve corresponds to the pump depletion in the 3WI case and the solid curve corresponds to the 5WI case. It is clear that for both SRS and SBS, the back reflectivity for the 5WI case is always lower than 3WI case (which is a well-known result in unmagnetized plasma (Sharma *et al.*, 2013; Vyas *et al.*, 2014*a*, *b*). It was expected because the intensity of the backscattered beams is directly proportional to the intensity of the incident pump beam and as the pump beam depletes the back reflectivity gets suppressed. In the 3WI case, pump depletion is less and hence the back reflectivity is always more than the 5WI case. It is also observed that for the *r*-mode back reflectivity of both the processes increases with the increasing background magnetic field, while for the *l*-mode back reflectivity of both the processes decreases with the increasing background magnetic field. In the presence of magnetic field, the interplay between SRS and SBS is a very complex process. The dynamical evolution of one scattering process is greatly affected by the interplay with the other coexisting process and by the magnetic field as well. Due to change in magnetic field or the interplay between the scattered beams, the gain factor of the respective backscattered beam (g_B and g_R) get modified, which further modifies the back-reflectivity. Therefore, the back reflectivity increases or decreases with increasing strength of the magnetic field.

At $B_0^0 = 15$ MG, for the *r*-mode Figure 3(a) and 3(b) represents the variation of back reflectivity of SBS and SRS with the plasma frequency, respectively while for the *l*-mode variation is represent by Figure 4(a) and 4(b). As observed, for both the scattering processes variation in plasma frequency

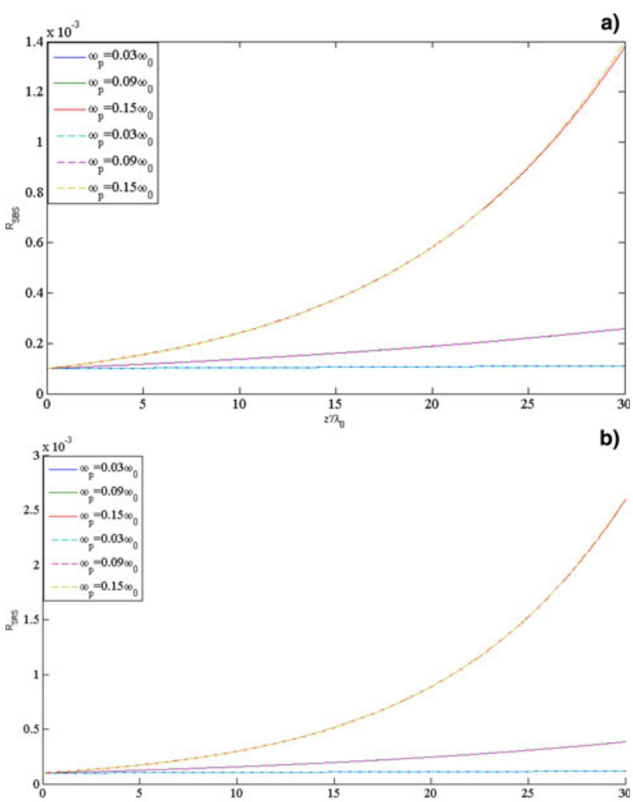

Fig. 3. Dependency of the back reflectivity of *r*-mode on the plasma frequency, (a) SBS process (R_{SBS}), (b) SRS process (R_{SRS}). The solid curve corresponds to the 5WI case and the dash curve corresponds to the 3WI case ($B_0^0 = 15$ MG).

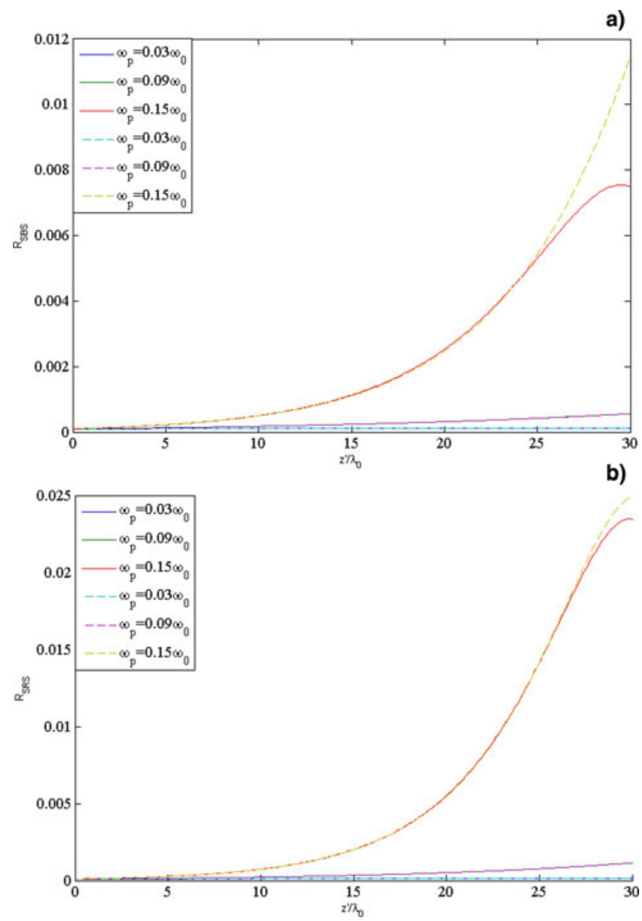

Fig. 4. Dependency of the back reflectivity of *l*-mode on the plasma frequency, (a) SBS process (R_{SBS}), (b) SRS process (R_{SRS}). The solid curve corresponds to the 5WI case and the dash curve corresponds to the 3WI case ($B_0^0 = 15$ MG).

https://doi.org/10.1017/S0263034616000720 Published online by Cambridge University Press

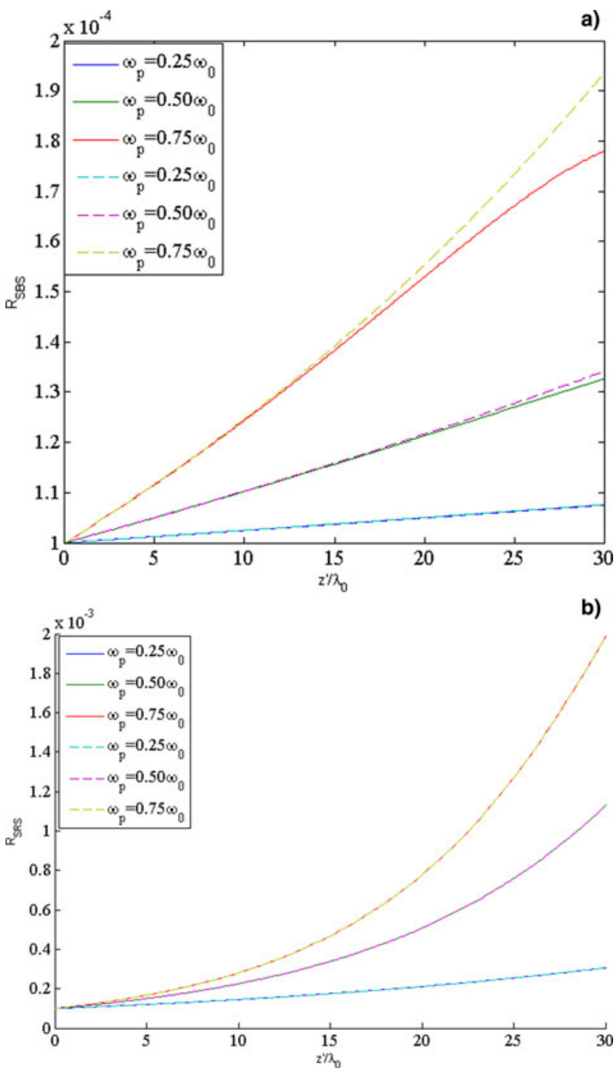

Fig. 5. Dependency of the back reflectivity of *l*-mode on the plasma frequency (above quarter critical density), (a) SBS process (R_{SBS}), (b) SRS process (R_{SRS}). The solid curve corresponds to the 5WI case and the dash curve corresponds to the 3WI case ($B_0^0 = 15\,MG$, $B_0^0 = 15\,\mathrm{MG}$, $\Gamma_e = 5 \times 10^{-2}\omega_0$, and $\Gamma_i = 10^{-4}\omega_0$).

greatly affect the back-reflectivities (R_{SBS} and R_{SRS}) and both of them get enhanced considerably due to the increasing plasma frequency for both *r*-mode as well as *l*-mode. Change in plasma frequency modifies the gain factors of the respective backscattered beam (g_B and g_R) and hence the back reflectivities (R_{SBS} and R_{SRS}) get enhanced accordingly. For both the scattering processes again the two cases; the 5WI case (solid curve) and 3WI case (dash curve) have been considered and in this situation also the back reflectivity in the 5WI case gets suppressed.

By combining dispersion relation of SRS wave [Eq. (2)] and Langmuir wave (same as in unmagnetized case) along with the phase-matching condition [Eq. (4)], it can be easily verify that for *l*-mode SRS can grow in the region higher than quarter critical density in the presence of external magnetic field. For the *l*-mode, Figure 5(a) and 5(b) represents the variation of back reflectivity of SBS and SRS with the plasma frequency, respectively, above the quarter critical density for $B_0^0 = 15\,\mathrm{MG}$. The solid curve represents the 5WI case and dash curve represents the 3WI case. As observed, in this situation also the back reflectivity of both the scattering processes get enhanced considerably due to the increasing plasma frequency and get suppressed due to coexistence of SRS and SBS (5WI).

4. CONCLUSION

In summary, we have carried out the interplay between two most important coexisting parametric instabilities, SRS and SBS in the presence of an axial magnetic field. We have derived and simulated the back reflectivity of both the scattering process and demonstrated the effect of coexistence phenomena (5WI) as well as the axial magnetic field on the back-reflectivity. We have observed that back reflectivity of one scattering process gets suppressed due to the presence of another (5WI case). Also, the variation in back reflectivity with the magnetic field and plasma frequency is observed, which demonstrates that as the strength of magnetic field increases the back reflectivity of both the scattering processes get supressed, whereas with the increasing plasma frequency back-reflectivities get enhanced.

ACKNOWLEDGMENTS

This work was partially supported by CSIR, India; UGC, India; and DST, India.

REFERENCES

Baeva, T., Gordienko, S. & Pukhov, A. (2006). Theory of high-order harmonic generation in relativistic laser interaction with overdense plasma. *Phys. Rev. E* **74**, 046404.

Barr, H.C., Berwick, S.J. & Mason, P. (1998). Six-wave forward scattering of short-pulse laser light at relativistic intensities. *Phys. Rev. Lett*. **81**, 2910.

Briand, J., Adrian, V., Tamer, M.El., Gomes, A., Quemener, Y., Dinguirard, J.P. & Kieffer, J.C. (1985). Axial magnetic fields in laser-produced plasmas. *Phys. Rev. Lett*. **54**, 38.

Chen, F.F. (1984). *Introduction to Plasma Physics and Controlled Fusion*. New York: Plenum Press.

Guérin, S., Laval, G., Mora, P., Adam, J.C., Heron, A. & Bendib, A. (1995). Modulational and Raman instabilities in the relativistic regime. *Phys. Plasmas* **2**, 2807.

Guérin, S., Mora, P. & Laval, G. (1998). Parametric instabilities due to relativistic electron mass variation. *Phys. Plasmas* **5**, 376.

Hao, L., Liu, Z.J., Hu, X.Y. & Zheng, C.Y. (2013). Competition between the stimulated Raman and Brillouin scattering under the strong damping condition. *Laser Part. Beams* **31**, 203.

Harding, A.K. & Lai, D. (2006). Physics of strongly magnetized neutron stars. *Rep. Progr. Phys*. **69**, 9.

Hellsten, T. & Villard, L. (1988). Power deposition for ion cyclotron heating in large tokamaks. *Nucl. Fusion* **28**, 285.

Khan, M., Das, C., Chakraborty, B., Desai, T., Pant, H.C., Srivastava, M.K. & Lawande, S.V. (1998*a*). Self-generated magnetic field and Faraday rotation in laser produced plasma. *Phys. Rev. E* **58**, 925.

Khan, M., Sarkar, S., Desai, T. & Pant, H.C. (1998*b*). Modification of stimulated Brillouin scattering due to magnetic anisotropy in laser plasma interaction. *Laser Part. Beams* **16**, 491.

Kolber, T., Rozmus, W. & Tikhonchuk, V.T. (1995). Saturation of backward stimulated Raman scattering and enhancement of laser light scattering in plasmas. *Phys. Plasmas* **2**, 256.

Kruer, W.L. (1974). *The Physics of Laser Plasma Interaction*. New York: Addison-Wesley.

Labaune, C., Baldis, H.A., Renard, N., Schifano, E. & Michard, A. (1997). Interplay between ion acoustic waves and electron plasma waves associated with stimulated Brillouin and Raman scattering. *Phys. Plasmas* **4**, 423.

Li, X.Y., Wang, J.X., Zhu, W.J., Ye, Y., Li, J. & Yu, Y. (2011). Enhanced inner-shell x-ray emission by femtosecond-laser irradiation of solid cone targets. *Phys. Rev. E* **83**, 046404.

Lindl, J.D., Amendt, P., Berger, R.L., Glendining, S.G., Glenzer, S.H., Hann, S.W., Kauffman, R.L., Landen, O.L. & Suter, L. (2004). The physics basis for ignition using indirect-drive targets on the National Ignition Facility. *Phys. Plasmas* **11**, 339.

Liu, C.S. & Tripathri, V.K. (1994). *Interaction of Electromagnetic waves with Electron beams and Plasmas*. Singapore: World Scientific.

Mahmoud, S.T. & Sharma, R.P. (2001). Effect of pump depletion and self-focusing (hot spot) on stimulated Raman scattering in laser-plasma interaction. *Laser Part. Beams* **64**, 613.

Michel, D.T., Depierreux, S., Stenz, C., Tassin, V. & Labaune, C. (2010). Exploring the saturation levels of stimulated Raman scattering in the absolute regime. *Phys. Rev. Lett*. **104**, 255001.

Mondal, S., Narayanan, V., Ding, W.J., Lad, A.D., Hao, B., Ahmad, S., Wang, W.M., Sheng, Z.M., Sengupta, S., Kaw, P., Das, A. & Kumar, G.R. (2012). Direct observation of turbulent magnetic fields in hot, dense laser produced plasmas. *Proc. Natl. Acad. Sci. USA* **109**, 8011.

Montgomery, D.S., Albright, B.J., Barnak, D.H., Chang, P.Y., Davies, J.R., Fiksel, G., Froula, D.H., Kline, J.L., Macdonald, M.J., Sefkow, A.B., Yin, L. & Betti, R. (2015). Use of external magnetic fields in hohlraum plasmas to improve laser-coupling. *Phys. Plasmas* **22**, 010703.

Nicolaï, P., Vandenboomgaerde, M., Canaud, B. & Chaigneau, F. (2000). Effects of self-generated magnetic fields and nonlocal electron transport in laser produced plasmas. *Phys Plasmas* **7**, 4250.

Nijmudin, Z., Tatarakis, M., Pukhov, A., Clark, E.L., Dangor, A.E., Fayre, J., Malka, V., Neely, D., Santala, M.I.K. & Krushelnick, K. (2001). Measurements of the inverse faraday effect from relativistic laser interactions with an underdense plasma. *Phys. Rev. Lett*. **87**, 215004.

Paknezhad, A. (2012). Effect of relativistic nonlinearity on the growth rate of Brillouin instability in the interaction of a short laser pulse with an underdense plasma. *Phys. Scr.* **86**, 065402.

Perkins, F.W. (1977). Heating tokamaks via the ion-cyclotron and ion-ion hybrid resonances. *Nucl. Fusion* **17**, 1197.

Remington, B.A., Drake, R.P., Takabe, H. & Arnett, D. (1999). Modeling astrophysical phenomena in the laboratory with intense lasers. *Science* **284**, 1488.

Sandhu, A.S., Dharmadhikari, A.K., Rajeev, P.P., Kumar, G.R., Sengupta, S., Das, A. & Kaw, P.K. (2002). Laser-generated ultrashort multimegagauss magnetic pulses in plasmas. *Phys. Rev. Lett*. **89**, 225002.

Sentoku, Y., Rahl, H., Mima, K., Tanaka, K.A. & Kishimoto, Y. (1999). Plasma jet formation and magnetic-field generation in the intense laser plasma under oblique incidence. *Phys. Plasmas* **6**, 2855.

Sharma, R.P. & Dragila, R. (1988). Effect of a self-generated dc-magnetic field on forward Raman scattering and hot electrons in laser produced plasmas. *Phys. Fluids* **31**, 1695.

Sharma, R.P., Vyas, A. & Singh, R.K. (2013). Effect of laser beam filamentation on coexisting stimulated Raman and Brillouin Scattering. *Phys. Plasmas* **20**, 102108.

Shuller, S. & Porzio, A. (2010). Order statistics and extreme properties of spatially smoothed laser beams in laser-plasma interaction. *Laser Part. Beams* **28**, 463.

Sodha, M.S., Sharma, R.P. & Kaushik, S.C. (1976). Interaction of intense laser beams with plasma waves: stimulated Raman scattering. *J. Appl. Phys*. **47**, 3518.

Srivastava, M.K., Lawande, S.V., Khan, M., Das, C. & Chakraborty, B. (1992). Axial magnetic field generation by ponderomotive force in a laser-produced plasma. *Phys. Fluids B* **4**, 4086.

Tajima, T. & Dawson, J.M. (1979). Laser electron accelerator. *Phys. Rev. Lett*. **43**, 267.

Tajima, T. & Mourou, G. (2002). Zettawatt–exawatt lasers and their applications in ultrastrong-field physics. *Phys. Rev. ST* **5**, 031301.

Vyas, A., Singh, R.K. & Sharma, R.P. (2014*a*). Combined effect of relativistic and ponderomotive filamentation on coexisting stimulated Raman and Brillouin scattering. *Phys. Plasmas* **21**, 112113.

Vyas, A., Singh, R.K. & Sharma, R.P. (2014*b*). Study of coexisting stimulated Raman and Brillouin scattering at relativistic laser power. *Laser Part. Beams* **32**, 657.

Vyas, A., Singh, R.K. & Sharma, R.P. (2016). Effect of the magnetic field on coexisting stimulated Raman and Brillouin back scattering of an extraordinary mode. *Phys. Plasmas* **23**, 012107.

Walsh, C.J., Villeneuve, D.M. & Baldis, H.A. (1984). Electron plasma-wave production by stimulated Raman scattering: competition with stimulated Brillouin scattering. *Phys. Rev. Lett*. **53**, 1445.

Wang, X., Krishnan, M., Saleh, N., Wang, H. & Umstadter, D. (2000). Electron acceleration and the propagation of ultrashort high-intensity laser pulses in plasmas. *Phys. Rev. Lett*. **84**, 5324.